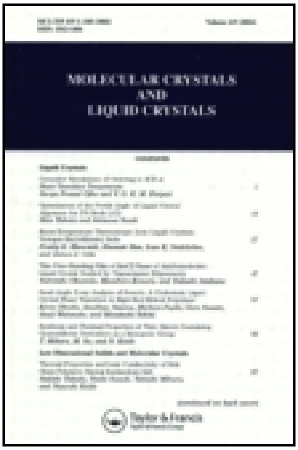

Molecular Crystals and Liquid Crystals
Publication details, including instructions for authors and subscription information:
http://www.tandfonline.com/loi/gmcl20

Experimental and Numerical Studies on Liquid Crystal Lens with Spherical Electrode

Bin Wang [a], Mao Ye [a] & Susumu Sato [a]
[a] Department of Electrical and Electronic Engineering, Akita University, Tegatagakuen-cho, Akita, Japan

Version of record first published: 31 Aug 2006

Mol. Cryst. Liq. Cryst., Vol. 433, pp. 217–227, 2005

ISSN: 1542-1406 print/1563-5287 online
DOI: 10.1080/15421400590957431

Taylor & Francis
Taylor & Francis Group

Experimental and Numerical Studies on Liquid Crystal Lens with Spherical Electrode

Bin Wang
Mao Ye
Susumu Sato
Department of Electrical and Electronic Engineering, Akita University, Tegatagakuen-cho, Akita, Japan

A liquid crystal lens with spherical electrode is studied experimentally and numerically. The power of the liquid crystal lens is dependent on the applied voltage. The measurements of the lens power are in agreement with the calculations. The size of the liquid crystal lens is that of the spherical electrode, and therefore can be changed arbitrarily.

Keywords: liquid crystal lens; phase profile; spherical electrode

INTRODUCTION

Liquid crystal (LC) materials have large electrical and optical anisotropies, and their optical properties can therefore be easily changed by external electric fields. LC materials are widely used in making electrooptic devices. Liquid crystal lenses are optical lenses made of LC materials. The advantage of the LC lens is that its focal length is tunable by an external electric field. Several types of LC lenses have been proposed [1–7].

The earliest proposal of LC lens is a lens-shaped LC lens [1]. The lens is fabricated by filling a nematic LC into a chamber formed by a glass lens and a glass substrate. The curved surfaces of the LC layer in the cell lead to some problems. Firstly, the response of the LC

This work was supported in part by Akita Prefecture Collaboration of Regional Entities for the Advancement of Technological Excellence, Japan Science and Technology Agency (JST).

Address correspondence to Susumu Sato, Department of Electrical and Electronic Engineering, Akita University, 1-1 Tegatagakuen-cho, Akita 010-8502, Japan. E-mail: satosu@ipc.akita-u.ac.jp

directors to the external electric field and the recovery of the directors after the field is removed change with location in the LC layer owing to the nonuniform thickness of the LC layer, and the response and recovery of the cell are very slow. Secondly, the directors usually do not rotate in one direction as an electric field is applied; in the rubbing direction, the directors at the two sides of the cell center tend to tilt up in opposite directions, and therefore a disclination line perpendicular to the rubbing direction is often observed [8,9]. The appearance of the dislination line is not desired, for it deteriorates the quality of the LC lens [10]. Thirdly, the alignment treatment on a curved surface is difficult, so the fabrication of the cell is complicated.

An LC microlens [2] is an LC lens with a planar LC layer. Its lens effect is produced by a nonuniform electric field. Hole-patterned electrodes are employed to form an axially symmetric nonuniform electric field in the LC layer. The LC microlens is demonstrated good lens quality [11]. The problem associated to this kind of structure is that the diameter of the lens is limited to only several hundreds of micrometers.

We have proposed an LC lens with a planar LC layer and a spherical electrode recently [12]. The lens size is equal to the size of the spherical electrode, and it is therefore changeable arbitrarily. In this paper, the LC lens is studied experimentally and numerically. The LC director reorientation is calculated. The calculated lens power that depends on the applied voltage is in agreement with the measurements.

LENS STRUCTURE

The structure of the LC lens is shown in Figure 1. A planar LC cell with homogenous alignment is used. The transparent electrodes are represented by the dark lines in the figure.

In the absence of an applied voltage, the LC directors are homogeneously aligned parallel to the x-axis in the LC cell. The LC cell shows no lens effects (Fig. 1(a)). When a voltage is applied across the two transparent electrodes, a nonuniform molecular reorientation is generated by the axially symmetric nonuniform electric field formed in the LC layer (Fig. 1(b)). A bell-like distribution of the refractive index can be obtained. Thus, the LC cell may act as an optical lens. Since the distribution of the tilt angles of the LC directors changes with the applied voltage, the phase profile of the incident light wave polarized in the x-axis, that is, an extraordinary wave, changes also with the applied voltage. Hence, the focal length of the LC lens is voltage dependent.

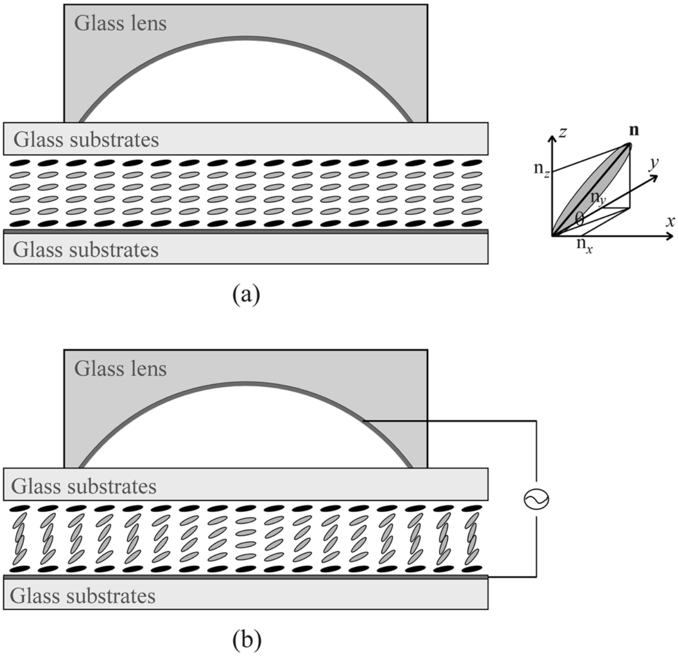

FIGURE 1 Structure of LC lens.

NUMERICAL CALCULATION

When a voltage is applied across the electrodes, a nonuniform electric field in the LC layer is generated since there is a thickness difference between the electrodes. In the LC layer, the total free energy is the minimum in the equilibrium state. The orientation of the LC directors $\boldsymbol{n} = (n_x, n_y, n_z)$ and the electric potential V should obey the Euler-Lagrange equation

$$-\frac{\partial f}{\partial u} + \frac{\partial}{\partial \beta}\left[\frac{\partial f}{\partial\left(\frac{\partial u}{\partial \beta}\right)}\right] = 0, \tag{1}$$

where u denotes n_x, n_y, n_z, or V, and β denotes x, y, or z. The electric field $\boldsymbol{E} = -\nabla V$. The free-energy density f includes electric and elastic ones, and can be expressed as [13]

$$f = \frac{1}{2}[K_{11}(\nabla \cdot \boldsymbol{n})^2 + K_{22}(\boldsymbol{n} \cdot \nabla \times \boldsymbol{n})^2 + K_{33}(\boldsymbol{n} \times \nabla \times \boldsymbol{n})^2] - \frac{1}{8\pi}(\varepsilon \cdot \boldsymbol{E}) \cdot \boldsymbol{E}, \tag{2}$$

where K_{11}, K_{22} and K_{33} are the splay, twist and bend elastic constants, respectively, ε the dielectric constant tensor of the LC and is $\varepsilon_{ik} = \varepsilon_{\perp}\delta_{ik} + (\varepsilon_{\|} - \varepsilon_{\perp})n_i n_k$ [14]. Here, $\varepsilon_{\|}$ and $\varepsilon_{\perp}$ are the dielectric constants of the LC parallel and perpendicular to the local LC directors, respectively. i, k denote x, y, or z. δ_{ik} is 1 if i equals k, and 0 otherwise. Strong anchoring on the upper and bottom walls is assumed.

Putting $\boldsymbol{n} = (n_x, n_y, n_z)$ and $\boldsymbol{E} = -\nabla V$ into Eq. (2), and substituting Eq. (2) into Eq. (1), the nonlinear differential equations for n_x, n_y, n_z and V in the LC layer are obtained. In the glass and air, the electric potential obeys the equation $\nabla^2 V = 0$. At the boundary of the liquid crystal layer and glass substrate, and at the boundary of the glass substrate and the air between the glass substrate and the glass lens, the electric displacement vector satisfies $D_n^{\mathrm{LC}} = D_n^{\mathrm{g}}$, and $D_n^{\mathrm{g}} = D_n^{\mathrm{air}}$, respectively [14], where D_n is the component of the vector $\boldsymbol{D} = \varepsilon \cdot \boldsymbol{E}$ along the outward normal to the surface. The finite difference method is used in the calculation [9]. At each calculation loop, $\boldsymbol{n}$ is normalized to maintain $|\boldsymbol{n}| = 1$ [15,16]. After solving $\boldsymbol{n}$, the local tilt angle θ of the LC directors can be obtained by the equation $\boldsymbol{n} = (n_x, n_y, n_z) = (\cos\theta\cos\phi, \cos\theta\sin\phi, \sin\theta)$, where ϕ is the azimuthal angle of the LC directors.

In the calculation the following values for the physical and geometrical parameters are used. The dielectric constant of the glass substrate (Matsunami Micro Cover Glass 0100) is $\varepsilon_g = 6.9$. The dielectric constants of the LC (Merck K15) are $\varepsilon_{\perp} = 5.9$ and $\varepsilon_{\|} = 18.2$. The elastic constants of the LC are $K_{11} = 6.7 \times 10^{-7}$ dyne, $K_{22} = 4.0 \times 10^{-7}$ dyne, and $K_{33} = 8.0 \times 10^{-7}$ dyne. The pretilt angle of the LC directors is $\theta_0 = 2.0°$. The thicknesses of the LC layer $t_{\mathrm{LC}} = 300\,\mu\mathrm{m}$ and the upper glass substrate $t_{\mathrm{sub}} = 300\,\mu\mathrm{m}$, respectively. The radius of curvature, and the center thickness of the glass lens (Sigma Koki SLB-10-100N) are 51.90 and 0.24 mm, respectively. The size of the glass lens is ϕ 10.0 mm. The voltage applied on the cell is normalized by $V_c = 2\pi(\pi K_{11}/\Delta\varepsilon)^{1/2}$. According the parameters listed above, $V_c = 0.78\,\mathrm{V}$.

At an applied voltage of $V_0 = 10\,\mathrm{V}$, the equipotential lines between the two electrodes in the plane $x = 0$ before director rotation are shown in Figure 2(a). In the figure the regions of $z = 0$–0.30 mm, 0.30–0.60 mm, and 0.60–0.84 mm represent the LC layer, the cover substrate, and the glass lens, respectively. The electric field concentrates in the air region between the glass lens and the upper glass substrate and distributes nonuniformly in the LC layer. In the LC the gradient electric field inside the aperture is the weakest at the center and the strongest around the edge. Figure 2(b) is the equipotential lines in the LC layer in the plane $z = t_{\mathrm{LC}}/2$. The electric field is nearly centrosymmetric.

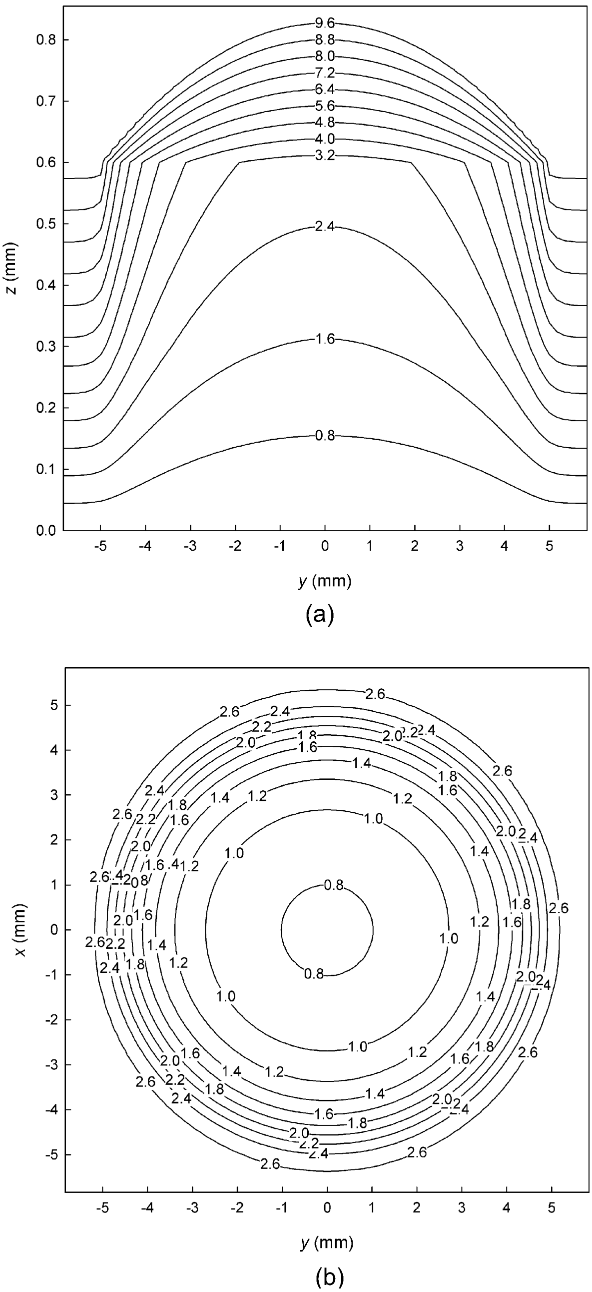

FIGURE 2 Equipotential lines. (a) In the plane $x = 0$. (b) In the plane $z = t_{LC}/2$.

The orientations of the LC directors in the plane $x = 0$ at $V_0 = 10$, 12, and 16 V are depicted in Figure 3. The tilt angles of the short bars in the figure represent that of the LC directors. The rotation of the LC directors near the edge is larger than that of the LC directors near the center, and the gradient distribution of θ changes with V_0.

The phase retardation φ experienced by an extraordinary wave from a He-Ne laser is

$$\varphi = \frac{2\pi}{\lambda}\int_0^{t_{LC}} \frac{n_o n_e}{(n_e^2 \sin^2\theta + n_o^2 \cos^2\theta)^{1/2}} dz. \tag{3}$$

In the equation, $\lambda = 0.633\,\mu m$ is the wavelength of the light wave, and $n_o = 1.533$ and $n_e = 1.707$ the ordinary and extraordinary refractive indices of the LC, respectively. φ at $V_0 = 10$, 12 and 16 V are shown in Figure 4. φ changes with V_0. Figure 5 shows φ in the plane $x = 0$ at different V_0. The triangles are calculations and the curves are fittings using equations $\varphi = \varphi_0 - (2\pi/\lambda)y^2/(2 \times 396)$ (for $V_0 = 10\,V$), $\varphi = \varphi_0 - (2\pi/\lambda)y^2/(2 \times 436)$ (for $V_0 = 12\,V$), and $\varphi = \varphi_0 - (2\pi/\lambda)y^2/(2 \times 557)$ (for $V_0 = 16\,V$), respectively, where φ_0 depends on the selection of the zero-phase position and the unit for length is millimeter. The equations take nearly the same form of the phase $\varphi = -(2\pi/\lambda)y^2/(2f)$ of a thin glass lens [17].

At $V_0 = 10$, 12, and 16 V, the LC layer can therefore be regarded as a lens of focal length of $f_{LC} = 396$, 436, and 557 mm, respectively. So the LC layer behaves like an optical lens with an electrically tunable focal length at a certain range of V_0.

EXPERIMENTAL

The LC lens with spherical electrode is realized experimentally. The nematic LC is Merck K15. The substrate surfaces contacting the LC are covered with polyimide films (Optmer AL1254 of Japan Synthetic Rubber Corporation) and rubbed in one direction. The LC directors are then aligned homogeneously in one direction in the LC cell. A glass lens of Sigma Koki SLB-10-100N is used and has the same geometry as that used in the numerical calculation.

To evaluate the properties of the LC lens, the profile of the phase retardation φ of the extraordinary wave is measured. The LC lens is placed between two crossed polarizers with a $\pi/4$ angle between the rubbing direction and the polarizers. The beam is from a He-Ne laser. The ordinary and extraordinary rays interfere. As the thickness of the LC layer is uniform, the ordinary wave retains its planar wave-front. The interference fringes at the exiting surface then show the phase

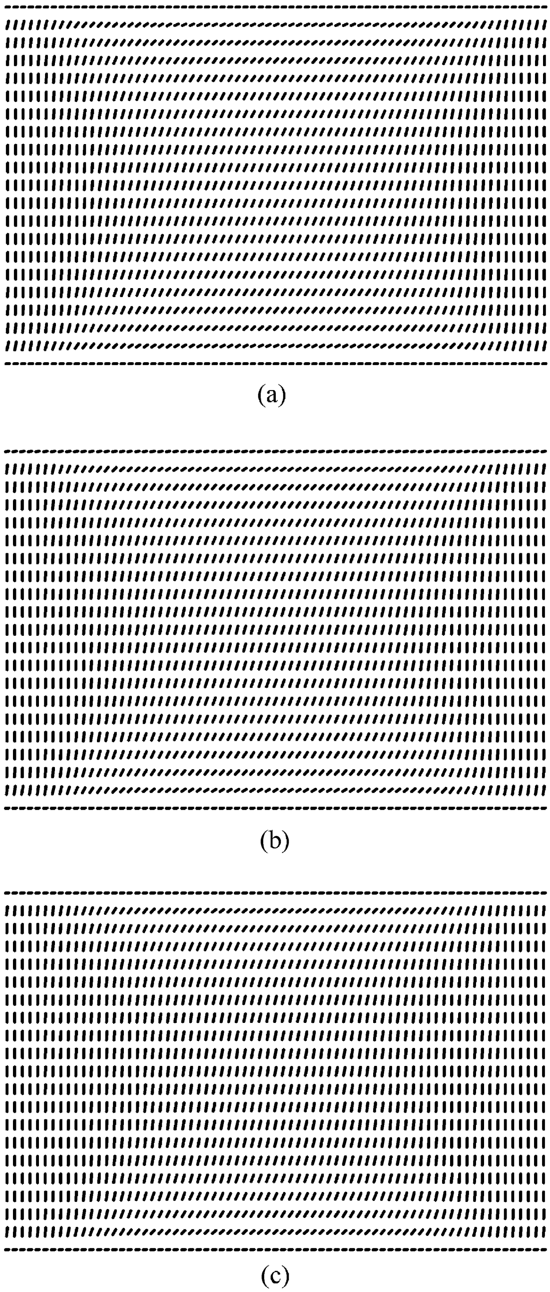

FIGURE 3 Reorientation of LC directors in the plane $x = 0$. (a) $V_0 = 10\,\text{V}$. (b) $V_0 = 12\,\text{V}$. (c) $V_0 = 16\,\text{V}$.

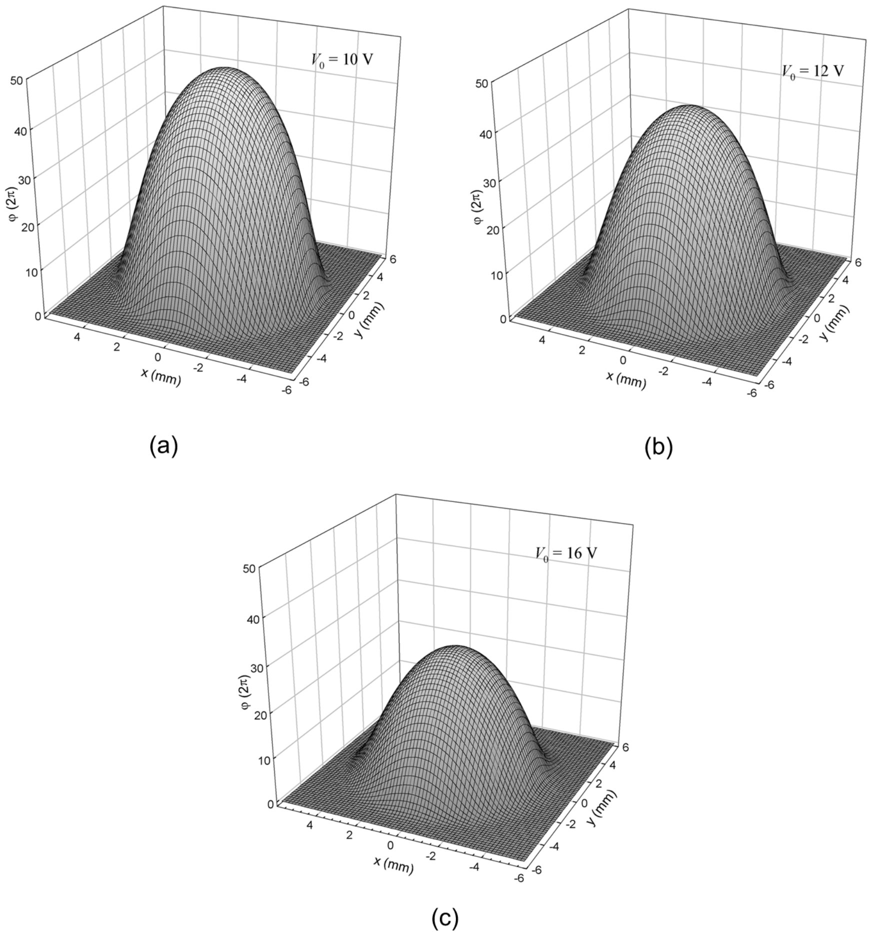

FIGURE 4 Phase profile. (a) $V_0 = 10\,\text{V}$. (b) $V_0 = 12\,\text{V}$. (c) $V_0 = 16\,\text{V}$.

profile of the extraordinary wave. There is a phase difference of 2π between two neighboring fringes.

The phase retardations at different voltages are obtained and the results are shown in Figure 6. The dots indicate measurements in the plane of $x = 0$ at $V_0 = 10$, 12, and 16 V_{rms}, and the solid curves quadratic fittings. The profile of φ is close to a quadratic form and changes with V_0. The measurements are in agreement with the calculations.

Figure 7 shows the power $P = 1/f$ of the LC lens as a function of V_0. The dots represent the experimental results and the curve the

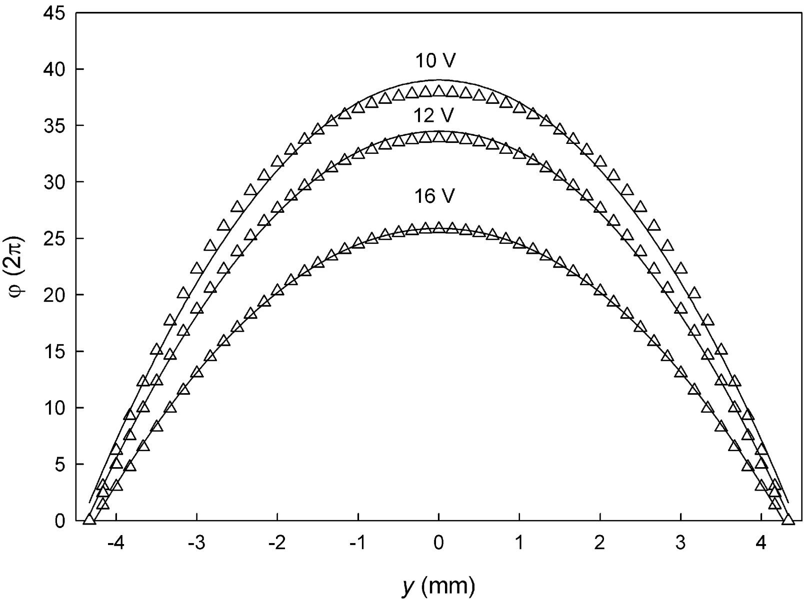

FIGURE 5 Calculations of phase profile in the plane $x = 0$.

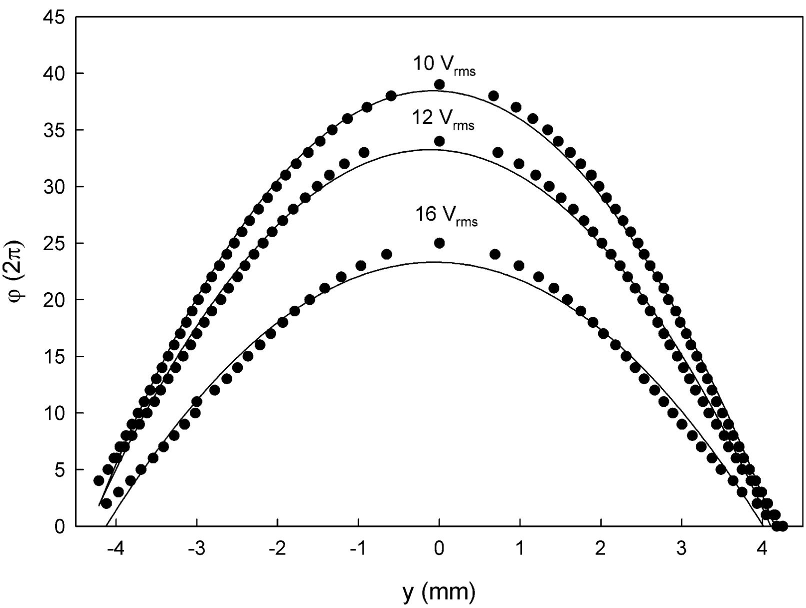

FIGURE 6 Measurements of phase profile in the plane $x = 0$.

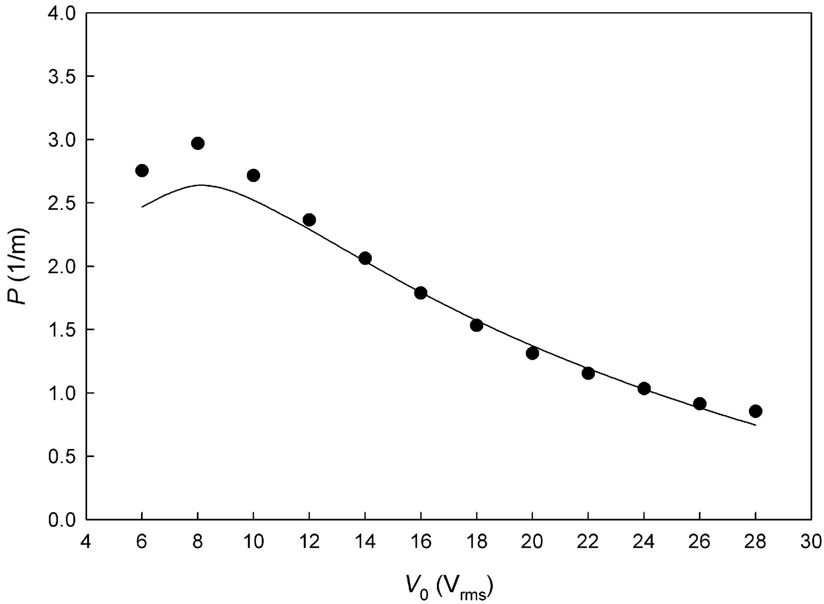

FIGURE 7 Power of LC lens changes with the applied voltage.

calculation. P first increases with V_0. After reaching a maximum value, it begins to decrease. The nonuniform director reorientation is the origin of the focusing property of LC lenses. The reorientation of the LC directors by the electric field near the edge is larger than that of the directors near the center. The difference of the reorientations increases with voltage when the voltage is small, and P increases. As V_0 becomes sufficiently high, the rotation of the directors near the edge approaches saturation, while the directors near the center continue to rotate with V_0, the spatial profile of reorientation flattens, and P of the LC lens decreases.

CONCLUSIONS

The LC lens with spherical electrode is studied experimentally and numerically. The reorientation of the LC directors and the phase profile of the incident light wave at different applied voltage are calculated. The property of the focus change is numerically simulated. The LC lens is fabricated and its properties are measured. The power of the LC lens is controllable by the applied voltage. The calculations are in agreement with the measurements.

REFERENCES

[1] Sato, S. (1979). *Jpn. J. Appl. Phys.*, *18*, 1679.
[2] Nose, T. & Sato, S. (1989). *Liq. Cryst.*, *5*, 1425.
[3] Riza, N. A. & DeJule, M. C. (1994). *Opt. Lett.*, *19*, 1013.
[4] Naumov, A. F., Loktev, M. Yu., Guralnik, I. R., & Vdovin, G. (1998). *Opt. Lett.*, *23*, 992.
[5] Ye, M. & Sato, S. (2002). *Jpn. J. Appl. Phys.*, *41*, L571.
[6] Ren, H. & Wu, S. T. (2003). *Appl. Phys. Lett.*, *82*, 22.
[7] Wang, B., Ye, M., & Sato, S. (2004). *Appl. Opt.*, *43*, 3420.
[8] Nose, T., Honma, M., & Sato, S. (2000). *Proc. SPIE.*, *4418*, 120.
[9] Wang, B., Ye, M., & Sato, S. (2004). *Mol. Cryst. Liq. Cryst.*, *413*, 423.
[10] Ye, M., Wang, B., & Sato, S. (2003). *Jpn. J. Appl. Phys.*, *42*, 5086.
[11] Nose, T., Masuda, S., & Sato, S. (1991). *Jpn. J. Appl. Phys.*, *30*, L2110.
[12] Wang, B., Ye, M., Honma, M., Nose, T., & Sato, S. (2002). *Jpn. J. Appl. Phys.*, *41*, L1232.
[13] de Gennes, P. G. (1974). *The Physics of Liquid Crystal*, Oxford, UP: London.
[14] Landau, L. D., Lifshitz, E. M., & Pitaevskii, L. P. (1995). *Electrodynamics of Continuous Media*, Butterworth-Heinemann Ldt, Oxford.
[15] Mori, H., Gartland, E. C. Jr., Kelly, J. R., & Bos, P. J. (1999). *Jpn. J. Appl. Phys.*, *38*, 135.
[16] Ye, M. & Sato, S. (2001). *Jpn. J. Appl. Phys.*, *40*, 6012.
[17] Goodman, J. W. (1968). *Introduction to Fourier Optics*, McGraw-Hill Book Company: San Francisco.